

A New Method for the Measurement of Low Concentrations of OH/O₂⁻ Radical Species in Water by High-LET Pulse Radiolysis. A Time-Resolved Chemiluminescence Study

V. Wasselin-Trupin,[†] G. Baldacchino,^{*,†} S. Bouffard,[‡] E. Balanzat,[‡] M. Gardès-Albert,[§] Z. Abedinzadeh,[§] D. Jore,[§] S. Deycard,^{||} and B. Hickel[†]

CEA/Saclay DSM/DRECAM/SCM URA 331 CNRS, Bât 546 91191 Gif/Yvette Cedex, France, and CIRIL (CEA-CNRS), rue Cl. Bloch, BP 5133, 14040 Caen Cedex, France, and Laboratoire de Chimie-Physique UMR 8601 CNRS, 45, rue des Saints Pères, 75270 Paris cédex 6, France, and UFR de Pharmacie, Bd Becquerel, 14032 Caen, France

Received: February 4, 2000; In Final Form: July 5, 2000

The new method described in this article allows the detection of low concentrations of radical species created in water for high linear energy transfer (LET) pulse radiolysis. The time-resolved chemiluminescence was used in a pulse radiolysis experiment at the Grand Accélérateur d'Ions Lourds (Caen, France) with an ⁴⁰Ar¹⁸⁺ ion beam for the determination of radical yields. In water, for an LET of 280 eV/nm, the yield of OH is 2.2 × 10⁻⁸ mol/J. A minimum value of the e_{aq}⁻ and HO₂/O₂⁻ yields is obtained. These experimental *G* values are compared to those obtained for the same LET. They are in good agreement with the values in the literature. The sensitivity of the time-resolved chemiluminescence method allows the measurement of concentrations of radicals species as low as 2 × 10⁻⁷ M.

Introduction

The linear energy transfer (LET = -dE/dx) effect in water radiolysis with high-energy particles has been phenomenologically understood for a long time.¹ The yields of radicals (H, OH, and e_{aq}⁻) decrease with increasing LET, which is explained in terms of radical recombinations due to the high concentration of radical species along the ionization tracks.^{2,3} These radical-radical reactions increase the yields of molecular species (H₂O₂ and H₂). An exception to this rule is the yield of the superoxide radical (HO₂/O₂⁻), which increases at high LET.^{4,5}

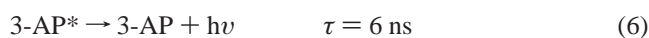
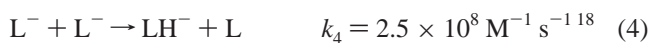
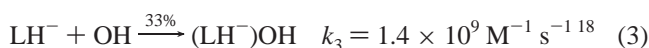
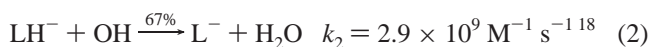
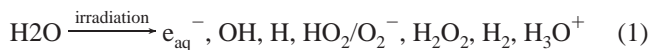
To simulate effects of high energy deposition in water, many calculations were performed with codes based mainly on a Monte Carlo model.⁶⁻⁸ To check and compare different models, it is essential to have experimental values of radiolytic yields at different values of LET. However, very few experimental data are available for high-LET irradiations. This is mainly due to the very low optical absorbances (low concentrations and low molecular absorption coefficients) attained in pulse radiolysis experiments with high-LET particles such as ions.^{2,4,9-11} However time-resolved absorption spectroscopy remains the best method for directly detecting radical species and measuring their concentrations, their rates of formation, and their rates of disappearance. Nevertheless, other methods are used to measure the radical yields, such as the scavenging method, in which a radical reacts specifically with a solute (scavenger) to yield a stable product that can be analyzed a long time after the irradiation.^{12,13} A variation of this method is to measure directly, by time-resolved absorption spectroscopy, the formation and decay of the product.¹⁴ The time dependence of the radical concentration can be recovered via a Laplace transformation

linking the concentration of the stable product, the concentration of the scavenger, and the rate constant of the reaction between the radical and the scavenger. Another method for analyzing the radical production in irradiated water is light emission spectroscopy, which is a very sensitive method for detecting excited states of molecules. This method has been used by LaVerne for the study of heavy-ion radiolysis of benzene, with a single-photon-counting technique.¹⁵

In this article, a new method for the detection of low concentrations of radical species in water is described. It is based on time-resolved light emission spectroscopy coupled to a scavenging method and chemiluminescence. Cyclic hydrazide molecules such as luminol (LH₂) are commonly involved in measurement of very low concentrations of hydrogen peroxide.¹⁶ Their reaction with OH and O₂⁻ radicals leads to a radiative excited state. This luminescence is used in our experiment in the quantitative analysis of low concentrations of radicals generated by irradiation with high-energy ⁴⁰Ar¹⁸⁺ pulses.

Principle

In this section, the luminol method is described. All rate constant values are taken from ref 17, unless otherwise specified. The reactions of luminol molecules with water radiolysis products are known.¹⁸ In the absence of O₂, the mechanism is:



* Author to whom correspondence should be addressed. E-mail: gbaldacchino@cea.fr. Fax: 01 69 08 34 66.

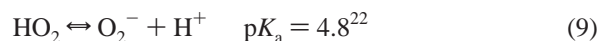
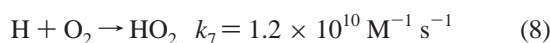
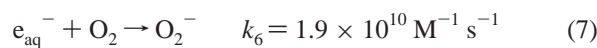
[†] CEA/Saclay DSM/DRECAM/SCM URA 331 CNRS.

[‡] CIRIL (CEA-CNRS).

[§] Laboratoire de Chimie-Physique UMR 8601 CNRS

^{||} UFR de Pharmacie.

In the presence of O₂, reactions 7–9 must be considered.

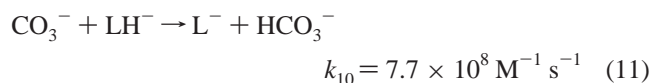
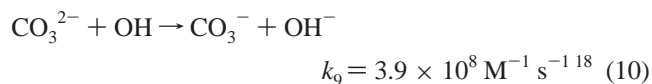


The hydroxyl radical (OH) reacts with the deprotonated form of luminol, LH⁻ (pK_a = 6.3) by reactions 2 and 3. The superoxide radical (O₂⁻) reacts with L⁻ by reaction 5 to give 3-aminophthalate (3-AP) in its first singlet excited state,¹⁸ which returns to its fundamental state with emission of a photon (λ_{max} = 420 nm, τ = 6 ns¹⁹). The chemiluminescence quantum yield of luminol is dependent on pH, and its maximum value is near pH 12.^{20,21}

This chemiluminescence mechanism requires the participation of two primary radicals of water radiolysis: OH and O₂⁻. A consequence is that, if the concentration of one of these radicals is lower than the other, this species limits the formation of 3-AP* and then of the intensity of chemiluminescence by either reaction 2 or reaction 5. Thus, the measurement of chemiluminescence gives the concentration of the radical that has the lowest concentration. Below an LET value of 100 eV/nm, the hydroxyl radical yield is higher than the superoxide radical yield. Over 100 eV/nm, the hydroxyl radical yield is lower than superoxide radical yield.¹ Then, this method allows for the measurement of the superoxide yield at low LET and of the hydroxyl yield at high LET.

The chemiluminescence needs to be calibrated by measuring the signal produced by a known concentration of radical. Then, it is necessary to know the quantity of light measured from a given concentration of superoxide radical in the solution. In aerated solutions, at low LET (as in the case of an electron beam), the superoxide radical is produced by the reaction of O₂ with e⁻_{aq} (reaction 7) and H (reaction 8). Under these conditions, the radical yields are known, and the concentration of the superoxide radical can be calculated.

Note that the mechanism presented in this article is the main mechanism for the luminol molecule. Actually, another pathway leading to the excited state molecule (3-AP*) exists, but only in the presence of O₂ and excess L⁻ (thus, excess of OH). In aerated solutions and under conditions leading to high OH yields, reaction 3 can indirectly produce luminescence. To avoid addition of OH radical onto the C=C bond (reaction 3), it is possible to use carbonate ions CO₃²⁻, with a sufficient concentration, to scavenge OH radicals (reaction 10); this forms CO₃⁻ radicals, which react with LH⁻ to give L⁻ (reaction 11).^{23,24}



In the case of high-LET irradiation and, then, under conditions leading to low OH yields, the luminescence initiated by reaction 3 can be neglected, and carbonate solutions become useless.

When the solution containing luminol and CO₃²⁻ is saturated by N₂O/O₂ mixtures, most of the e⁻_{aq} are scavenged by N₂O (reaction 12) to give additional OH radicals. In this case G(OH) > G(O₂⁻), and the intensity of chemiluminescence is proportional to the concentration of O₂⁻ produced by the reaction of

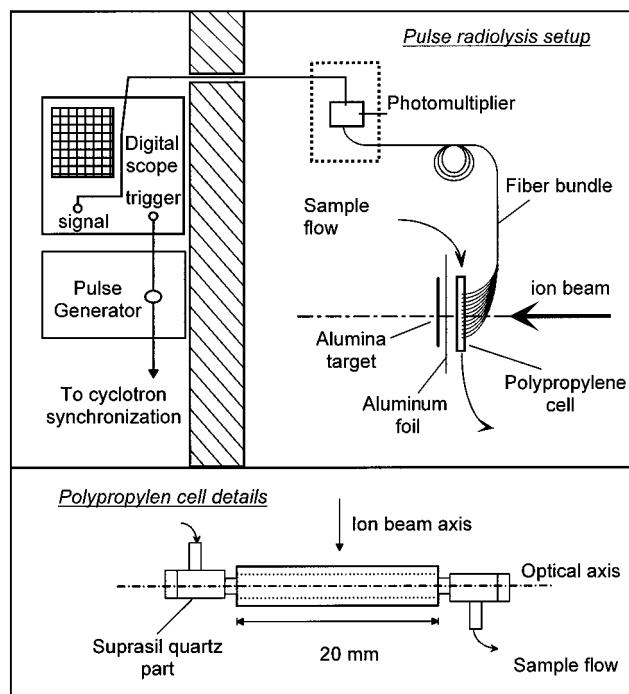
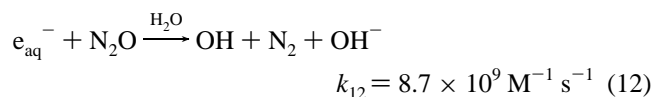


Figure 1. Setup scheme of the time-resolved chemiluminescence experiment with ion beam.

O₂ with H and the small fraction of e⁻_{aq} that is not scavenged by N₂O (reaction 7). Thus, a calibration can be done, providing that the cell is irradiated uniformly.



To summarize this principle, one can measure the low radical yields a short time after a pulsed irradiation with high-LET particles by measuring chemiluminescence.

Experimental Method

Ion Beam. Pulsed irradiations were performed with an ⁴⁰Ar¹⁸⁺ ion beam of energy 95 MeV/nucleon (which gives 3.8 GeV/ion) at the Grand Accélérateur National d'Ions Lourds (GANIL) cyclotron. The setup is depicted in Figure 1. The irradiation cell is a cylindrical flow cell, made of polypropylene to avoid a luminescence background from quartz (material commonly used in such experiments). The thickness of the polypropylene is 0.5 mm, allowing an almost-constant LET (280 ± 31 eV/nm) into the total thickness of the sample (3 mm). The LET is calculated from the TRIM compilation.²⁵

The section geometry of the ion beam is defined by a horizontal slit in front of the cell. The beam intensity is measured with a secondary electron detector located in the beam. It consists of a thin titanium foil placed between two thin aluminum foils. A potential of 48 V applied to these aluminum foils creates an electric field that generates an easily measured current. This intensity is calibrated before the actual irradiations with a Faraday cup. The same device has been used in previous experiments.⁹ The dose delivered to the sample is then calculated by the energy loss of the ion in the water and the intensity of the beam.

The ion beam has intrinsically one pulse of 1 ns duration every 100 ns. However, a pulse generator is used to modulate this high frequency, and it generates a burst of pulses having a duration of between 5 μs and 2 ms at a frequency of 20 Hz.

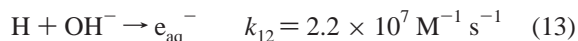
Optical System and Data Acquisition. Chemiluminescence is collected by a bundle of optical fibers (Figure 1). The light is led to a photomultiplier (R928S, Hamamatsu). The signal is digitized by a numerical scope (TDS 680B Tektronix). To improve the signal-to-noise ratio and to maintain the time resolution at the microsecond time scale, an impedance of 100 k Ω or 10 k Ω is connected in parallel with the input of the 1-M Ω impedance of the scope. Fifty triggered signals were accumulated to improve the signal-to-noise ratio. During the acquisition, the solution is changed by a flow system (1 mL/s).

Because of the solid angle for the light collection and for the light detection, the distances from the fiber to the cell and from the fiber to the photomultiplier must remain exactly the same for all experiments, especially when the calibration and the real experiments are achieved with different accelerators (see calibration section).

Aqueous Solutions. The solutions were prepared using ultrapure water (Millipore Alpha Q, 18.2 M Ω cm, 10 ppb of total organic carbon). The pH was adjusted to pH 12 with sodium hydroxide (Aldrich, 99.99%). The sodium salt of 3-aminophthalhydrazide (luminol, Sigma) was used for preparation of a 10⁻³ M luminol solution. For the calibration, K₂CO₃ (Merck, pro analysis) was added.

Solutions were deaerated by bubbling with high purity argon (99.999%). Other gases were dissolved in some solutions: N₂O (99.998%) or mixture of N₂O/O₂ (20% and 10%).

Calibration. Calibration was performed with a Febetron 707 accelerator delivering 2 MeV electrons in a single pulse of 10 ns duration. In the presence of known concentrations of oxygen, the reaction of oxygen with hydrated electrons and H atoms generates a known quantity of HO₂/O₂⁻ species. Dosimetry was performed with a solution of KSCN saturated with N₂O by measuring the absorption of (SCN)₂⁻: a He-Ne laser (543.5 nm) measures optical absorption along the optical axis of the cell (see the details of the cell in Figure 1). The dose in grays is calculated by using $\epsilon_{543.5} = 3900 \text{ M}^{-1} \text{ cm}^{-1}$ ²⁶ and $G[(\text{SCN})_2^-] = 6.39 \times 10^{-7} \text{ mol/J}$.²⁷ For the calibration, only low doses have been used (between 1 and 100 Gy) in order to avoid biradical reactions occurring with high-dose-rate irradiations. The concentration of emitting species 3-AP is proportional to the concentration of O₂⁻ produced by radiolysis of aqueous solution containing luminol (0.001 M), CO₃²⁻ (0.01 M), and saturated with N₂O/O₂ mixtures. The mixtures used were 10% O₂ and 20% O₂. At pH 12, there is a competition for H atoms between reactions 8 and 13. In the case of e_{aq}⁻, the competition is between O₂ and N₂O (reactions 7 and 12).



The concentration of O₂⁻ is expressed in eq 14 as a function of the dose in grays and of the fraction of H ($A_{10\% \text{O}_2} = 88 \pm 2\%$; $A_{20\% \text{O}_2} = 93 \pm 1\%$) and e_{aq}⁻ ($B_{10\% \text{O}_2} = 1.2 \pm 0.05\%$; $B_{20\% \text{O}_2} = 2.6 \pm 0.15\%$) that reacts with O₂

$$[\text{O}_2^-] = \text{Dose}[AG_{\text{H}} + BG_{\text{e}_{\text{aq}}^-}] \quad (14)$$

where $G_{\text{H}} = 5.7 \times 10^{-8}$ and $G_{\text{e}_{\text{aq}}^-} = 3.1 \times 10^{-7}$ are the primary yields of, respectively, H and e_{aq}⁻ expressed in moles per joule.

In the case of calibration with an electron beam, the Cerenkov light is very intense and depends on the dose delivered by the pulse. The signal of Cerenkov light is included in the light detected and superposed on the luminescence signal (Figure 2). The Cerenkov signal corresponds to 33% of the total signal. The Cerenkov light is subtracted from the total signal. The luminescence signal is then integrated as a function of time in

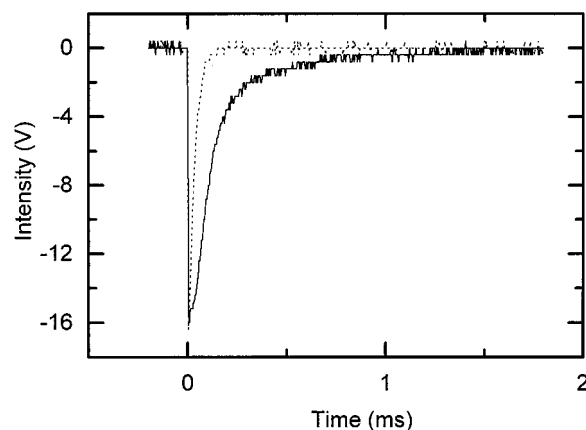


Figure 2. Intensity of light as a function of time in a solution of luminol at pH 12 irradiated with electron beam: —, total light emitted; - - -, Cerenkov light.

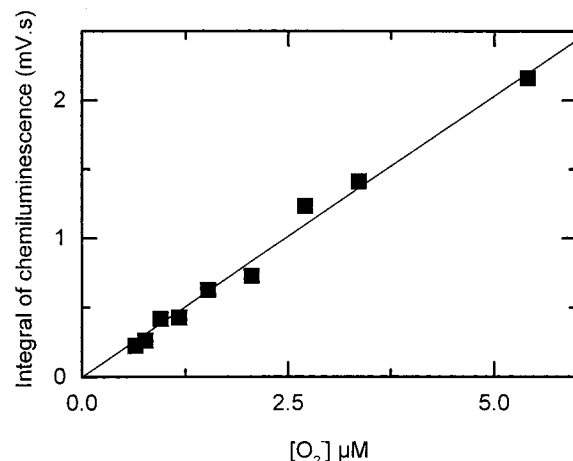


Figure 3. Calibration curve of the intensity of chemiluminescence as a function of the concentration of the chemiluminescent 3-AP molecules formed.

order to take into account all of the reactions producing luminescence during the diffusion period after the pulse irradiation. For several doses, corresponding to several concentrations of O₂⁻, the integral of the chemiluminescence signal is plotted in Figure 3. The regression curve is then obtained as

$$\text{Icl} (\text{V s}^{-1}) = 406 (\text{V M}^{-1} \text{ s}^{-1}) \times [\text{O}_2^-] (\text{M}) \quad (15)$$

where Icl is the integral of the chemiluminescence signal.

Results

Signals. Figure 4 presents the emission of light as a function of time when a solution containing 10⁻³ M luminol at pH 12 is irradiated by an ⁴⁰Ar¹⁸⁺ ion beam. This curve is the result of 50 averaged signals at a repetition rate of 20 Hz. The origin of time corresponds to the entrance of the ion pulse into the cell. The emission of light begins during the pulse and reaches its maximum at 10 μs (which is the duration of the pulse used in the experiment). The lifetime of fluorescence is 6 ns. This cannot explain that the duration of the light intensity decay is 300 μs . A simulated curve, obtained by a radiolysis software CHEMSIMUL²⁸, is plotted in Figure 4. Rather good agreement is obtained between the experimental and simulated curves, considering that simulated curve is obtained without adjusting the rate constants taken from the literature.¹⁷ The input file contains the reactions involving the species of water radiolysis

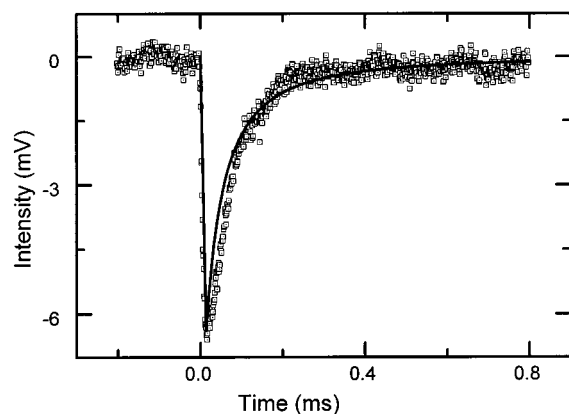


Figure 4. Emission of light as a function of time in a solution of luminol at pH 12 deaerated, irradiated with heavy-ion beam: □, experimental curve; —, simulated curve.

with their rate constants, the reactions involving luminol, and the radiative rate constant of 3-AP*. This confirms that the decay of the light intensity was due to the rate constant of the reaction of L^- with O_2^- (reaction 5).

The integral of the signal was proportional to the concentration of emitting species, 3-AP*, and to the concentration of limiting radical, OH or O_2^- . For every acquisition, the integral of the signal was plotted against the dose delivered. Three different solutions were irradiated: aerated, deaerated, and saturated with N_2O . The results obtained were similar for the aerated and deaerated solutions. From solutions saturated with N_2O , the intensity of chemiluminescence was larger.

Yield Determination. With eq 15, the integral of chemiluminescence was transformed into the concentration of emitting species. These concentrations are plotted versus the dose for the different experiments in Figure 5. The slope of the linear regression gives the yield of emitting species formed, in moles per joule.

The results are

$$G_{\text{aerated}}(3\text{-AP}^*) = 1.6 \times 10^{-8} \text{ mol/J}$$

$$G_{\text{deaerated}}(3\text{-AP}^*) = 1.4 \times 10^{-8} \text{ mol/J}$$

$$G_{\text{N}_2\text{O saturated}}(3\text{-AP}^*) = 2.7 \times 10^{-8} \text{ mol/J}$$

The G value in deaerated solutions is close to the G value in aerated solutions. In N_2O -saturated solution, the G value is increased by almost a factor of 2.

Aerated and Deaerated Solutions. With high-LET irradiation, as in this experiment, O_2^- is a primary radical of water radiolysis. In deaerated solutions, the yield of O_2^- is expressed by the primary radical yield (eq 16). When the solution is aerated, the e_{aq}^- and H primary yields are added to the primary yield of the radical (eq 17), because O_2^- is formed by reactions 7 and 8.

$$G_{\text{deaerated}}(O_2^-) = G_{O_2^-} \quad (16)$$

$$G_{\text{aerated}}(O_2^-) = G_{O_2^-} + G_{e_{\text{aq}}^-} + G_{\text{H}} \quad (17)$$

However, in our experiments, the G values of the emitting species are found to be similar in aerated and deaerated samples. It can therefore be deduced that the concentration of emitting species is not proportional to the superoxide radical concentration because this would imply that $G_{e_{\text{aq}}^-} + G_{\text{H}}$ is close to zero.

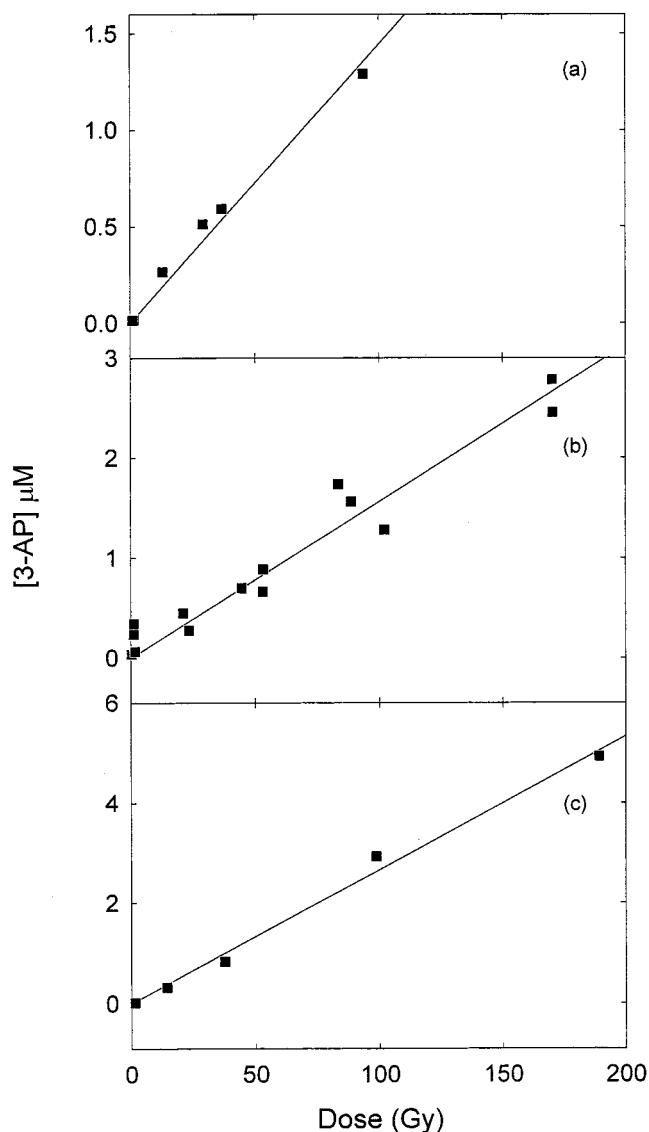
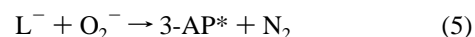
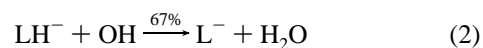


Figure 5. Concentration of emitting species versus the dose for an irradiation by heavy-ion beam of a solution containing 10^{-3} M luminol at pH 12: (a) aerated solution, (b) deaerated solution, (c) N_2O -saturated solution.

In the mechanism of chemiluminescence of luminol under irradiation, two equations are important.



The hydroxyl radical and the superoxide radical are involved in reactions 2 and 5. If the concentration of one of these radicals is lower than that of the other, this radical limits the chemiluminescence. The concentration of emitting species is equal to the concentration of this limiting species. In our case, the limiting species cannot be the superoxide radical because the experimental G values obtained in aerated and deaerated solutions are equal. The limiting species should be the radical OH, and the luminescence intensity is proportional to its concentration. According to reactions 2 and 3, the radical yield measured corresponds to 67%, which is equal to the ratio of rate constants k_2 and k_3 of the OH radical produced: $g(\text{OH}) = 2.2 \times 10^{-8} \text{ mol/J}$.

N_2O -Saturated Solutions. In solutions saturated with N_2O , O_2 is removed, and the yield of O_2^- is expressed only by its

primary yield $g(\text{O}_2^-)$. According to reaction 5, $G(\text{O}_2^-)$ is at least equal to $G(3\text{-AP})$, and then equal to $G_{\text{N}_2\text{O saturated}}(3\text{-AP})$. Actually, the yield determination reveals that $G_{\text{N}_2\text{O saturated}}(3\text{-AP})$ is greater than $G_{\text{deaerated}}(3\text{-AP})$, which confirms that the limiting species in aerated and deaerated solutions is not O_2^- but OH. From this experiment, it can be concluded that $g(\text{O}_2^-) \geq 2.7 \times 10^{-8}$ mol/J.

In reaction 12, e_{aq}^- is transformed into OH, which can react with luminol to give the diazasemiquinone and enhance the chemiluminescence yield obtained in previous experiments, where OH was the radical limiting the reaction 2. The yield of luminescence $G_{\text{N}_2\text{O}}(3\text{-AP})$ in the N_2O -saturated solutions corresponds to the minimum value of 67% of the OH radical produced: $G(\text{OH}) = g(\text{OH}) + g(e_{\text{aq}}^-) \geq 4 \times 10^{-8}$ mol/J. The difference between the yields of OH obtained in deaerated and N_2O -saturated water gives $g(e_{\text{aq}}^-) \geq 2.5 \times 10^{-8}$ mol/J.

Discussion

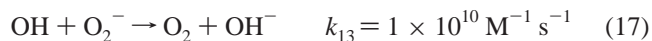
Sensitivity. Using absorption spectroscopy, the detection limit for O_2^- , which has ϵ of $2000 \text{ M}^{-1}\text{cm}^{-1}$ at 260 nm,²² is approximately 5×10^{-6} M. By time-resolved chemiluminescence, 4×10^{-8} M of superoxide radical was easily measured. The very good signal-to-noise ratio could allow measurements of lower concentrations of superoxide radical. The sensitivity of the chemiluminescence is greater than that of previous absorption spectroscopy.

Hydroxyl Radical. The primary yield of hydroxyl determined in our experiments (2.2×10^{-8} mol/J) is close to the results of other recent experiments under high-LET conditions of irradiation. This latter value corresponds to the yield of OH scavenged by 10^{-3} M luminol according to reaction 2. The scavenging capacity, which is $k_X[X]$, where X in our case is luminol and k_X is k_2 , is equal to $2.9 \times 10^9 \text{ M}^{-1} \text{ s}^{-1}$. Earlier experiments were performed at almost the same scavenging capacity. Formic acid was used by Burns et al.,³ La Verne,¹² and Baldacchino et al.⁹ to measure the hydroxyl primary yield. La Verne found a yield around 3×10^{-8} mol/J, for a scavenging capacity of $1.3 \times 10^6 \text{ s}^{-1}$ at an LET of 230 eV/nm. Similar results were obtained by Baldacchino et al.: $g(\text{OH}) = (2 \pm 0.2) \times 10^{-8}$ mol/J, for a scavenging capacity of $3.2 \times 10^6 \text{ s}^{-1}$ at an LET of 250 eV/nm. Because of a higher LET (280 eV/nm) than in these latter experiments, our $g(\text{OH})$ value (2.2×10^{-8} mol/J) remains in good agreement with the latter literature values. Our result is also in good agreement with the results obtained by Burns et al.³ [$g(\text{OH}) = 4.2 \times 10^{-8}$ mol/J at LET of 140 eV/nm, $g(\text{OH}) = 1.9 \times 10^{-8}$ mol/J at LET of 650 eV/nm] for a scavenging capacity of $3.2 \times 10^7 \text{ s}^{-1}$. These values are higher than our value, but this discrepancy can be explained by the scavenging capacity being higher too. Thus, in their case, OH is scavenged earlier by formate and has less time to react with the other radicals and molecular products of water radiolysis.

Superoxide Radical. A minimum value of the superoxide radical primary yield has been measured: $g(\text{O}_2^-) \geq 2.7 \times 10^{-8}$ mol/J. This value is higher than that obtained by Burns et al.³ and Baldacchino et al.⁹ In the experiments of Burns and Sims,³ the superoxide radical yield is 8.4×10^{-9} mol/J at LET = 140 eV/nm and 1.9×10^{-8} mol/J at LET = 650 eV/nm. Baldacchino et al. have determined $g(\text{O}_2^-) = 6 \times 10^{-9}$ mol/J by direct observation of superoxide radical after a pulse of 2 ms of ³⁶S¹⁶⁺ ion beam at LET = 250 eV/nm. Our value is higher than the values in the literature.

In our experiment, a competition exists between the reaction of luminol with OH (reactions 2 and 3) and the reaction of OH with superoxide radical (reaction 17). Considering the

high concentration of luminol used (10^{-3} M), OH reacts essentially with luminol. Then, superoxide radical is protected from the attack of OH.



In time-resolved absorption spectroscopy, water without OH scavenger was used, so superoxide radical is not protected from the attack of OH (reaction 17). An estimation using a homogeneous kinetics simulation by CHEMSIMUL shows that, after a pulse of 2 ms, the superoxide yield at 2 ms represents only 40% of the primary superoxide yield. This estimation underestimates the disappearance of O_2^- at short times when the radical distribution is not homogeneous. During the pulse, part of the superoxide radical population has disappeared by reaction with OH (reaction 17). This can explain the difference between our result and the values obtained by absorption spectroscopy.^{3,9}

Hydrated Electron. In this experiment, a minimum value of the hydrated electron primary yield can be obtained by comparison of the solution saturated with N_2O , where $G(\text{OH}) = g(\text{OH}) + g(e_{\text{aq}}^-)$. The scavenging capacity of N_2O is then $2.2 \times 10^8 \text{ s}^{-1}$ because of reaction 12 giving OH radicals that participate in the luminol scavenging mechanism. As explained in the previous Superoxide Radical section, the totality of O_2^- is not scavenged. Thus, it is not possible to give the exact yield of O_2^- , and as a consequence, $g(e_{\text{aq}}^-)$ cannot be deduced. Only a minimum value can be calculated: $g(e_{\text{aq}}^-) \geq 2.5 \times 10^{-8}$ mol/J. At an LET value (250 eV/nm) similar to that of our experiment, Baldacchino et al.⁹ found $g(e_{\text{aq}}^-) = 5 \times 10^{-9}$ mol/J at a scavenging capacity of $3.2 \times 10^6 \text{ s}^{-1}$. The difference between these two results is due to the much higher scavenging capacity in N_2O solution, which corresponds to the yield of e_{aq}^- at 3 ns. Our result is in agreement with the expected decrease in $g(e_{\text{aq}}^-)$ when LET increases.¹

Conclusion

The time-resolved chemiluminescence method can provide measurements of lower concentrations of radicals in water than can time-resolved absorption spectroscopy. This method is recommended for irradiation with high-LET particles, if they have enough energy to ensure a constant LET in the irradiation cell.

Concentrations of OH/ O_2^- radicals down to 4×10^{-8} M have been measured. The radiolytic yields [$g(\text{OH}) = 2.2 \times 10^{-8}$ mol/J, $g(\text{O}_2^-) \geq 2.7 \times 10^{-8}$ mol/J, and $g(e_{\text{aq}}^-) \geq 2.5 \times 10^{-8}$ mol/J] for an LET of 280 eV/nm have been determined and compared to the literature values.

Acknowledgment. The authors thank the personnel of CIRIL (Centre Interdisciplinaire de Recherche Ions Lasers) and GANIL (Grand Accélérateur Nationale d'Ions Lourds) for technical assistance.

References and Notes

- (1) Allen, A. O. *The radiation chemistry of water and aqueous solutions*; Van Nostrand: New York, 1961.
- (2) Sauer, M. C.; Schmidt, K. H.; Hart, E. J.; Naleway, C. A.; Jonah, C. D. *Radiat. Res.* **1977**, *70*, 91–106.
- (3) Burns, W. G.; Sims, H. E. *J. Chem. Soc., Faraday Trans 1* **1981**, *77*, 2803–2813.
- (4) Sauer, M. C.; Schmidt, K. H.; Jonah, C. D.; Naleway, C. A.; Hart, E. J. *Radiat. Res.* **1978**, *70*, 519–528.
- (5) LaVerne, J. A.; Schuler, H.; Burns, W. G. *J. Phys. Chem.* **1986**, *90*, 3238–3242.
- (6) Frongillo, Y.; Fraser, M.-J.; Cobut, V.; Goulet, T.; Jay-Gerin, J. P.; Patau, J. P. *J. Chim. Phys.* **1996**, *93*, 93–102.

- (7) Cobut, V.; Frongillo, Y.; Patau, J. P.; Goulet, T.; Fraser, M.-J.; Jay-Gerin, J.-P. *Radiat. Phys. Chem.* **1998**, *51*, 229–243.
- (8) Frongillo, Y.; Goulet, T.; Fraser, M.-J.; Cobut, V.; Patau, J. P.; Jay-Gerin, J.-P. *Radiat. Phys. Chem.* **1998**, *51*, 245–254.
- (9) Baldacchino, G.; LeParc, D.; Hickel, B.; Gardès Albert, M.; Abedinzadeh, Z.; Jore, D.; Deycard, S.; Bouffard, S.; Mouton, V.; Balanzat, E. *Radiat. Res.* **1998**, *149*, 128–133.
- (10) Baldacchino, G.; Bouffard, S.; Balanzat, E.; Mouton, V.; Albert, M. G.; Abedinzadeh, Z.; Jore, D.; Deycard, S.; Parc, D. L.; Hickel, B. *J. Chim. Phys.* **1997**, *94*, 200–204.
- (11) Baldacchino, G.; Bouffard, S.; Balanzat, E.; Gardès Albert, M.; Z., A.; Jore, D.; Deycard, S.; Hickel, B. *Nucl. Instrum. Methods Phys. Res. B* **1998**, *146*, 528–532.
- (12) LaVerne, J. A. *Radiat. Res.* **1989**, *118*, 201–210.
- (13) LaVerne, J. A.; Yoshida, H. *J. Phys. Chem.* **1993**, *97*, 10720–10724.
- (14) Chitose, N.; LaVerne, J. A.; Katsumura, Y. *J. Phys. Chem. A* **1998**, *102*, 2087–2090.
- (15) LaVerne, J. A. *J. Phys. Chem.* **1996**, *100*, 18757–18763.
- (16) Olsson, B. *Anal. Chim. Acta* **1982**, *136*, 113–119.
- (17) Ross, A. B.; Mallard, W. G.; Helman, W. P.; Buxton, G. V.; Huie, R. E.; Neta, P. *NDRL–NIST Solution Kinetics Database*, version 2.0; NIST: Gaithersburg, MD, 1994.
- (18) Lee, J.; Seliger, H. H. *Photochem. Photobiol.* **1970**, *11*, 247–258.
- (19) Haas, Y.; Würzberg, E. *J. Phys. Chem.* **1979**, *83*, 2692–2696.
- (20) Lee, J.; Seliger, H. H. *Photochem. Photobiol.* **1972**, *15*, 227–237.
- (21) Merényi, G.; Lind, J. S. *J. Am. Chem. Soc.* **1980**, *102*, 5830–5835.
- (22) Bielski, B. H. J.; Cabelli, D. E.; Arudi, R. L. *J. Phys. Chem. Ref. Data* **1985**, *14*, 1041–1051.
- (23) Eriksen, T. E.; Lind, J.; Merényi, G. *J. Chem. Soc., Faraday Trans I* **1983**, *79*, 1503–1511.
- (24) Lind, J.; Merényi, G.; Eriksen, T. E. *J. Am. Chem. Soc.* **1983**, *105*, 7655–7661.
- (25) Ziegler, J. F.; Biersack, J. P.; Littmark, U. *Stopping power and ranges of ions in matter*; Pergamon Press: New York, 1985; Vol. 1.
- (26) Dogliotti, L.; Hayon, E. *J. Phys. Chem.* **1968**, *72*, 1800–1807.
- (27) Schuler, R. H.; Hartzell, A. L.; Behar, B. *J. Phys. Chem.* **1981**, *85*, 192–199.
- (28) Kirkegaard, P.; Bjergbakke, E. *CHEMSIMUL: a simulation for chemical kinetics*; RISO-R-395: Roskilde, Denmark, 1999.